Development 136, 3185-3193 (2009) doi:10.1242/dev.032334

Connexin 43 regulates epicardial cell polarity and migration in coronary vascular development

David Y. Rhee[1,*,†], Xiao-Qing Zhao[1,*], Richard J. B. Francis[1], Guo Ying Huang[3], John D. Mably[2] and Cecilia W. Lo[1,‡]

Connexin 43 knockout (Cx43 KO) mice exhibit conotruncal malformations and coronary artery defects. We observed epicardial blisters in the Cx43 KO hearts that suggest defects in epicardial epithelial-mesenchymal transformation (EMT), a process that generates coronary vascular progenitors. Analysis using a three-dimensional collagen gel invasion assay showed that Cx43 KO epicardial cells are less invasive and that, unlike wild-type epicardial cells, they fail to organize into thin vessel-like projections. Examination of Cx43 KO hearts using Wt1 as an epicardial marker revealed a disorganized pattern of epicardial cell infiltration. Time-lapse imaging and motion analysis using epicardial explants showed a defect in directional cell migration. This was associated with changes in the actin/tubulin cytoskeleton. A defect in cell polarity was indicated by a failure of the microtubule-organizing center to align with the direction of cell migration. Forced expression of Cx43 constructs in epicardial explants showed the Cx43 tubulin-binding domain is required for Cx43 modulation of cell polarity and cell motility. Pecam staining revealed early defects in remodeling of the primitive coronary vascular plexuses in the Cx43 KO heart. Together, these findings suggest an early defect in coronary vascular development arising from a global perturbation of the cytoarchitecture of the cell. Consistent with this, we found aberrant myocardialization of the outflow tract, a process also known to be EMT dependent. Together, these findings suggest cardiac defects in the Cx43 KO mice arise from the disruption of cell polarity, a process that may be dependent on Cx43-tubulin interactions.

KEY WORDS: Epicardium, Connexin 43, Heart development, Coronary vessels, Mouse

INTRODUCTION

Gap junctions are cell junctions containing membrane channels that mediate the passive diffusion of ions, metabolites and cell signaling molecules (Goldberg et al., 2002; Kanno and Saffitz, 2001; Wei et al., 2004; Saez et al., 2003). They comprise proteins encoded by a multigene family known as the connexins. The connexin protein Cx43, encoded by the gap junction gene *Gja1*, is abundantly expressed in the heart, where it mediates the electrical synchronization of myocardial contraction. Surprisingly, Cx43 knockout (KO) mice exhibit neonatal lethality associated with outflow tract obstruction and conotruncal pouches (Reaume et al., 1995). An abundance of ectopic vascular smooth muscle and endothelial cells are observed distributed in a disorganized manner, together with a variety of coronary artery patterning defects (Li et al., 2002; Walker et al., 2005; Clauss et al., 2006). These findings suggest that dysregulation of coronary vascular development plays a central role in the cardiac phenotype of the Cx43 KO mouse.

Studies using transgenic and Cx43 KO mice have suggested these cardiac defects might arise from perturbations involving two migratory cell populations, the cardiac neural crest and the epicardial cell lineages (Ewart et al., 1997; Huang et al., 1998a; Huang et al., 1998b; Sullivan and Lo, 1995; Xu et al., 2001). Both cell populations are derived by epithelial-mesenchymal transition (EMT), with cardiac neural crest emerging from the dorsal neural fold, and epicardial cells being derived from proepicardial progenitors (PE) situated near the septum transversum. Both migrate to the heart, and both are required for normal coronary vascular development. Cardiac neural crest cells do not directly contribute to formation of the coronary arteries, but are required for normal coronary patterning by regulating the organization and development of the coronary arteries (Hood and Rosenquist, 1992; Waldo et al., 1994). By contrast, the epicardially derived cells (EPDCs) give rise to vascular smooth muscle, and endothelial cells of the coronary vasculature (Poelmann et al., 1993; Mikawa and Gourdie, 1996; Dettman et al., 1998; Gittenberger-de Groot et al., 1998; Manner, 1999; Vrancken Peeters et al., 1999; Munoz-Chapuli et al., 2002; Zhou et al., 2008). Coronary arteries do not form in the absence or following the loss of the epicardium, such as in α4 integrin or Pecam KO mice (Kwee et al., 1995; Yang et al., 1995). Of significance to note, experimental manipulations that delayed deployment of the epicardium in chick embryos resulted in pouch-like structures in the heart and enlarged ectopic vessels reminiscent of the cardiac malformations of the Cx43 KO mouse (Perez-Pomares et al., 2002). These findings suggest defects in the deployment of EPDCs may play a pivotal role in the cardiac defects of the Cx43 KO mouse.

We previously showed that cells derived from E9.5 PE explants from Cx43 KO mouse embryos exhibit altered cell motility (Li et al., 2002). The PE originates from the splanchnic mesoderm situated near the septum transversum (Viragh and Challice, 1981). PE derivatives migrate on to the heart and rapidly spread to form the epicardium. A subset of epicardial cells then undergoes EMT, infiltrating the heart to generate vascular smooth muscle, fibroblasts and endothelial cells. The finding of abnormal PE cell migration suggests defects in the epicardium might contribute to the cardiac defects observed in the Cx43 KO mouse. The epicardium of near term or newborn Cx43 KO mouse hearts exhibits a striking change

[1]Laboratory of Developmental Biology, National Heart Lung and Blood Institute, National Institutes of Health, Bethesda, MD 20892, USA. [2]Department of Cardiology, Children's Hospital Boston and Department of Genetics, Harvard Medical School, Boston, MA 02115, USA. [3]Children's Hospital Cardiovascular Center, Children's Hospital of Fudan University, Shanghai 200032, China.

*These authors contributed equally to this work
†Present address: Department of Cardiology, Children's Hospital Boston and Department of Genetics, Harvard Medical School Boston, MA, USA
‡Author for correspondence (loc@nhlbi.nih.gov)

Accepted 14 July 2009

in morphology that suggests that abnormal epicardial EMT might underlie the dysregulation of coronary vascular development (Walker et al., 2005). To examine this question, in this study we analyzed epicardial cell migration and invasion in the Cx43 KO mouse heart between E11.5 and E13.5. By using Wt1 as an epicardial marker, we examined infiltration of EPDCs into the Cx43 KO heart, and we evaluated epicardial EMT using a collagen gel invasion assay. We also quantitatively assessed the migratory behavior of migrating epicardial cells in epicardial explants using time-lapse video microscopy. Together, these studies showed Cx43 plays a crucial role in modulating epicardial EMT and the deployment of EPDCs during cardiovascular development. We have further shown that this is likely to involve regulation of the cytoskeleton and cell polarity by Cx43. Using Cx43 expression constructs, we explored the requirement for a previously identified tubulin-binding domain in the carboxy terminus of Cx43 in the modulation of cell polarity (Giepmans et al., 2001a; Giepmans et al., 2001b). Cx43-tubulin interaction has been shown to mediate Cx43 trafficking to the cell membrane, and microtubules are also observed to preferentially target Cx43 gap junction plaques to the cell surface (Giepmans et al., 2001a; Lauf et al., 2002; Shaw et al., 2007). Expression of a Cx43 construct (Cx43dT) without the tubulin-binding domain caused a loss of epicardial cell polarity. Together, these findings suggest that cardiac defects in the Cx43 KO mice arise from the disruption of cell polarity, a process that might be dependent on Cx43-tubulin interactions.

MATERIALS AND METHODS

Mouse breeding and genotyping

Cx43 KO embryos were generated from interbreeding heterozygous Cx43 KO mice maintained in the C57BL6/J strain background. The protocol used for genotyping was modified as previously reported (Reaume et al., 1995). Timed pregnancies were obtained for embryo harvest, with the day a vaginal plug was detected being designated embryonic day 0.5 (E0.5).

Immunohistochemistry

For whole-mount Pecam immunohistochemistry, E13.5 hearts were fixed in 4% paraformaldehyde (PFA) for 4 hours, dehydrated in a methanol series, incubated in methanol/hydrogen peroxide, rehydrated, and blocked in PBSST (5% rabbit serum/PBS, 0.1% Triton X-100). The hearts were subsequently incubated with rat anti-mouse CD31 antibodies (BD Pharmingen, 1:200) followed by biotinylated rabbit anti-rat IgG antibody (Vector Laboratories, 1:200). The Vectastain Elite ABC Kit and DAB visualization (Vector Laboratories) were used to detect the bound antibodies. Antibody and ABC reagent incubations were carried out overnight at 4°C, then washed five times for 1 hour each wash at 4°C with PBSST. The hearts were examined and photographed using a Leica MZ 12.5 stereomicroscope equipped with ProgRes JENOPTIK C14 Plus digital camera.

For immunostaining of tissue sections, hearts were paraffin-wax embedded after 4% PFA fixation, and 7 μm sections were collected and processed for staining. Antigen retrieval was carried out in citrate buffer. Sections were blocked in 10% goat serum/PBS, then incubated with primary antibody: rabbit anti-cow Cytokeratin WSS (DakoCytomation, 1:100), rabbit anti-Wt1 (Thermo Scientific, 1:200) or mouse anti-α-Sarcomeric actin (Sigma, 1:400). This was followed by incubation with biotinylated goat anti-rabbit IgG (Vector Laboratories, 1:200) with the Vectastain Elite Kit and visualization by DAB or TrueBlue (KPL) detection. FITC-conjugated donkey anti-mouse secondary antibody (Jackson ImmunoResearch, 1:200) was used to visualize sarcomeric actin. The slides were examined using a Leica DMRE upright microscope equipped with a Hamamatsu Micromax CCD camera.

Three-dimensional collagen gel invasion assay

Collagen gels (1.2%) were adapted from a previously reported protocol (Runyan and Markwald, 1983). Type I rat tail collagen (BD Biosciences) was mixed with 10×M199 (Gibco), sterile water and 2.2% sodium bicarbonate. Gels were allowed to solidify in a four-well chamber (Nalge Nunc International) for 30 minutes at 37°C and then rinsed three times for 15 minutes each rinse with DMEM (Gibco). Gels were then conditioned overnight at 37°C in DMEM supplemented with 10% fetal bovine serum (Hyclone), insulin, transferrin, selenium-X (Gibco) and penicillin/streptomycin (Gibco). E11.5 hearts were dissected and the atria and outflow tract were removed. The hearts were then allowed to attach and grow out on the gel for 2 days, after which the hearts were removed and the explants cultured for another 2 days in media with serum. Following this incubation, cells were fixed in 4% PFA and permeabilized with Triton X-100. The explants were then stained with rhodamine-phalloidin (Molecular Probes, 1:200) and DAPI. Images were taken using either a Leica TCS LSI confocal microscope or a Leica DM LFSA upright microscope with a 40×water immersion objective and an Orca-ER CCD camera. To measure cell invasion depth, *z*-stacks were taken through the thickness of each collagen gel and the deepest 20 cells were measured relative to the surface of the explant. Six explants taken from three different litters were used for each genotype, with 120 cells for each genotype overall. Statistics were analyzed by ANOVA using Statview (SAS Institute, Cary, NC, USA). Three-dimensional digital reconstruction was created using Volocity software (Improvision, Coventry, England).

Two-dimensional epicardial explants and time-lapse video microscopy

E11.5 hearts were dissected and explanted into eight-well chamber slides (BD Falcon pre-coated with type I rat tail in DMEM supplemented with 10% fetal bovine serum and penicillin/streptomycin for 24-48 hours. For the transfection experiments, explants were transfected at 24 hours with 200 ng DNA/well using Opti-MEM I without serum, lipofectamine LTX and PLUS reagent (Invitrogen). For time-lapse imaging, the DMEM was replaced with Phenol Red-free L-15 (Gibco) media supplemented with 10% fetal bovine serum and penicillin/streptomycin. The cells were placed on a heated stage, maintained at 37°C and imaged at 3-minute intervals for 3 hours using a Leica DMIRE2 inverted microscope fitted with an Orca-ER camera. Individual cells were traced from the resulting time-lapse movies and analyzed using Dynamic Imaging Analysis Software (Solltech, Oakdale, IA, USA); a number of different cell parameters were calculated. The speed and directionality of cell movement was obtained by tracking the change in the position of the centroid of the cell at each time point. Roundness, defined as $100\times4\pi$ (area/perimeter^2) (Stites et al., 1998), is a measure of how efficiently a perimeter encloses an area. A circle has the largest area for a given perimeter with a roundness of 100%, while a straight line has a roundness of 0%. Thus, the greater the number of cell protrusions, the lower the roundness. Cell protrusions and retractions are measured as percent cell area formed versus lost as a cell migrates. Convexity and concavity is a measure of the complexity of cell shape. Line segments connecting the final shape of a cell are drawn and the angles of turning from one segment to the next are measured (Soll, 1995). Counter-clockwise turns are considered positive, while clockwise turns are considered negative. Convexity is the sum of positive turn angles in degrees and concavity is the sum of negative turn angles in degrees. All of the data obtained were evaluated by ANOVA using Statview (SAS Institute).

Immunocytochemistry

Epicardial explants were fixed in either 4% PFA or cold methanol for 10 minutes, then incubated with 0.15% Triton X-100 for 20 minutes and immunostained. The slides were incubated for 2 hours at room temperature with mouse anti-α-Tubulin (Sigma, 1:1000), rabbit anti-γ-Tubulin (Sigma, 1:500), mouse anti-GM130 (BD Pharmingen, 1:100) or rabbit anti-ZO-1 antibodies (Invitrogen, 1:100) diluted in blocking buffer (1% BSA, 5% FBS and 0.01% Triton X-100 in PBS). After washing three times with PBS for 15 minutes or longer, the slides were incubated with secondary antibody for 45 minutes at room temperature, then mounted using Vectashield-mounting medium with DAPI (Vector Laboratories). The staining was examined by epifluorescence illumination using a Leica DMRE upright microscope and images were captured using a 5 MHz Micromax cooled CCD camera.

Analysis of MTOC orientation

E11.5 epicardial cells were cultured for 2 days, then fixed and immunostained with an antibody to α-tubulin, or double immunostained with antibodies to γ-tubulin and the GM130 Golgi marker to visualize the microtubule organizing center (MTOC). Cells in the outer three cell layers of the emerging explant were analyzed for the orientation of the MTOC. Non-forward facing cells were scored using a previously described method (Magdalena et al., 2003; Nobes and Hall, 1999). Briefly, a clock face is over laid on the cell with a 120° sector aligned with the direction of cell migration. Cells in which the MTOC did not localize within this 120° sector facing the direction of cell migration were counted as being non-forward facing.

Real-time PCR

RNA was extracted from E11.5 epicardial explants cultured for 48 hours using the RNeasy Mini Kit (Qiagen) and was further amplified by the WT-Ovation System (Nugen). Real-time PCR was performed using an ABI 7500 real-time PCR instrument. Gene-specific primers and SYBR green/ROX qPCR master mix were obtained from SuperArray Bioscience. Amplification specificity was monitored using melting curve analysis. Normalization to the glyceraldehyde-3-phosphate dehydrogenase (GAPDH) expression level was used to control for input RNA concentrations. The data obtained were analyzed statistically using a two-sample *t*-test.

RESULTS

Epicardial blisters and alterations in the actin cytoskeleton

As epicardial EMT and infiltration of EPDCs into the myocardium play an essential role in formation of the coronary vasculature, we examined the epicardium in the E11.5 and E12.5 KO heart, shortly after the epicardium is fully delaminated, covering the entire heart, and during the time of active epicardial EMT and EPDC migration. In the KO hearts, abnormal epicardial and subepicardial blisters were observed (Fig. 1B,H). These corresponded to regions where the epicardium appeared to have detached from the underlying extracellular matrix. The cells in these blisters expressed cytokeratin, indicating that they are of epicardial origin (Fig. 1D).

To ascertain whether alterations in the actin cytoskeleton and focal adhesions might contribute to formation of the epicardial blisters, we generated epicardial explants from E11.5 Cx43 KO and wild-type hearts, and used rhodamine-phalloidin and vinculin antibody staining to examine the distribution of actin stress fibers and focal adhesion contacts, respectively. In wild-type epicardial cells, the actin filaments were typically aligned with the direction of cell migration (Fig. 2A), but in KO explants, the actin fibers were often not aligned with the direction of cell migration (Fig. 2C). Focal adhesions, structures that mediate cell-matrix attachment and to which actin stress fibers are anchored, were more abundant but smaller in size in the KO epicardial cells than in the wild type (Fig. 2B,D).

We also examined the distribution of ZO-1 (also known as Tjp1), a protein that interacts with the actin cytoskeleton and is known to directly bind Cx43 (Barker et al., 2002; Giepmans and Moolenaar, 1998; Giepmans et al., 2001b; Imamura et al., 1999; Itoh et al., 1997). The shuttling of ZO-1 between the membrane and the cytoplasm is suggested to play a role in EMT associated with tumor invasion (Polette et al., 2007). In wild-type epicardial cells, ZO-1 was localized at the cell surface, mainly along regions of cell-cell contact (Fig. 3A). In KO epicardial cells, the distribution of ZO-1 appeared more diffuse, with some cells showing significant cytoplasmic ZO-1 localization. In addition, the pattern of cell

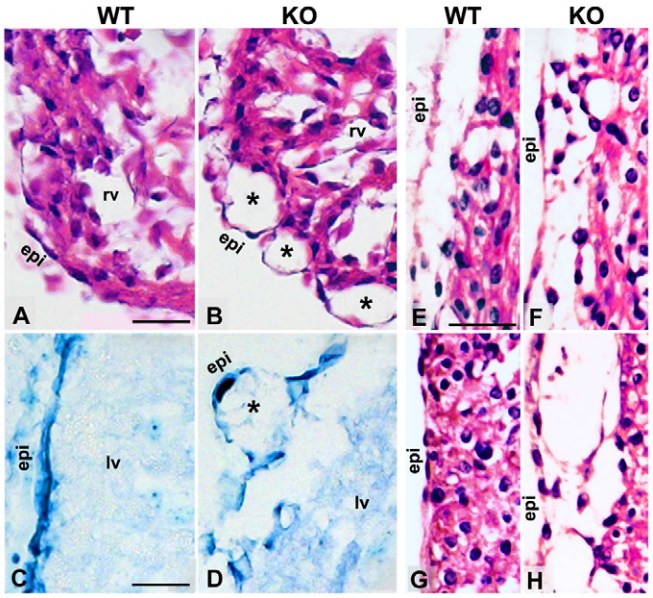

Fig. 1. Epicardial blisters in Cx43 KO mouse hearts. (**A-D**) Histological sections of E11.5 (A,B) right ventricle and E12.5 (C,D) left ventricle show the epicardial morphology of wild-type (A,C) and Cx43 KO (B,D) mouse hearts. Note the striking epicardial blisters seen in the KO heart (asterisks, B,D). (C,D) Cytokeratin staining of cells in the blisters indicates these are likely to be of epicardial origin. (**E-H**) Histological sections of the left ventricle (E,F) and apex (G,H) of hearts from E15.5 wild-type and Cx43 KO mice. Note the epicardial blisters in the KO hearts. WT, wild type; KO, knockout; epi, epicardium; rv, right ventricle; lv, left ventricle. Scale bars: 50 μm in A,E; 25 μm in C.

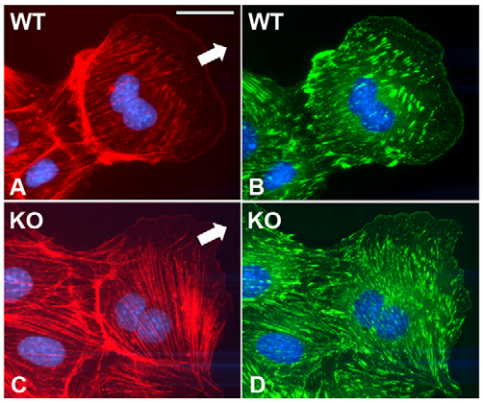

Fig. 2. Cx43 KO epicardial cells exhibit a defect in actin cytoskeleton organization. (**A-D**) The actin cytoskeleton and focal adhesion contacts in wild-type and Cx43 KO epicardial cells from E11.5 epicardial explant cultures were visualized with rhodamine-conjugated phalloidin (A,C, red) and vinculin antibody (B,D, green). Wild-type cells (A,B) show actin stress fibers aligned with the direction of cell migration (indicted by arrow in A), and dense actin filaments delineate the regions of cell-cell contact. By contrast, in the KO cells, the actin stress fibers were often not oriented with the direction of cell migration (indicated by arrow in C), and the density of actin filaments was reduced at regions of cell-cell contact. In these same cells, vinculin immunostaining showed prominent adhesion plaques in the wild-type epicardial cells (B). By contrast, KO epicardial cells have finer adhesion plaques (D). Scale bar in A: 10 μm.

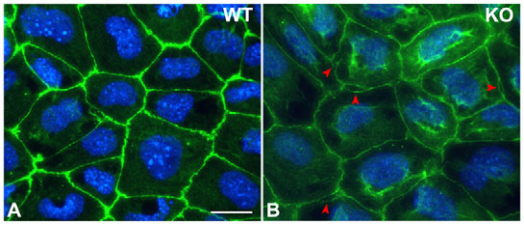

Fig. 3. Altered distribution of ZO-1 in Cx43 KO epicardial explants. (**A**,**B**) E11.5 epicardial explant cultures were immunostained with ZO-1 (green) antibody. Strong cell surface localization was observed at regions of cell-cell contract in wild-type epicardial cells (A). In Cx43 KO explants (B), ZO-1 localization at the cell surface was reduced concomitant with ZO-1 redistribution to the cytoplasm. The ZO-1 staining pattern in the KO epicardial explant showed many regions of apparent discontinuity in the epithelial sheet (arrowheads). Scale bar in A: 30 μm.

surface ZO-1 localization suggested a frequent detachment of cell-cell contacts in the KO epicardial sheets (see arrowheads in Fig. 3B). Together, these findings suggest a fundamental change in the organization of the actin cytoskeleton in the Cx43 KO heart, changes that might contribute to formation of the epicardial blisters.

Analysis of epicardial EMT and EPDC migration

To examine whether epicardial EMT is altered in the Cx43 KO heart, we used a three-dimensional (3D) collagen gel invasion assay to assess epicardial explants from E11.5 KO and wild-type embryos. Explants were obtained from six wild-type and six KO embryos derived from three independent litters. Epicardial cells emerging from the wild-type explants typically coalesced into well-organized, long, thin vessel-like projections in the 3D collagen gel (Fig. 4A). By contrast, the KO explants never showed such vessel-like projections (Fig. 4B). Analysis of these explants by confocal imaging and deconvolution microscopy provided 3D reconstructions that allowed the measurement of cell invasion depth into the collagen gel matrix (Fig. 4C-F). Cell penetration along the *z*-axes was ascertained for 120 cells from the wild-type and 120 cells from the KO explants. This analysis showed a significant reduction in invasion depth in the KO explants (Fig. 4G) compared with wild type. Together, these observations suggest that the Cx43 KO epicardial cells undergo EMT, but that the invading EPDCs are less invasive and do not align and organize properly.

To observe epicardial EMT and infiltration of EPDCs in vivo, we used Wt1 immunostaining to visualize invading EPDCs in the E13.5-E15.5 Cx43 KO and wild-type mouse hearts. Abundant Wt1-positive cells were observed in the epicardium and the subepicardial layers, and deeper in the underlying myocardium of both the KO and wild-type hearts (Fig. 5). In wild-type hearts, the invading EPDCs exhibited an elongate cell morphology that was aligned with the apparent direction of cell invasion into the heart (Fig. 5A,C). By contrast, Wt1-positive cells in the KO hearts showed a disorganized distribution with no consistent orientation (Fig. 5B,D). Interestingly, abundant EPDCs were also found lining the infundibulum, especially in the pouch forming regions (arrows in Fig. 5D).

By using quantitative real-time PCR, we examined the expression of genes known to play a role in EMT, including *Snail1/2*, E-cadherin, *Wt1* and *Tbx18*, but none showed any significant changes (see Table S1 in the supplementary material). This would suggest that EMT itself is not fundamentally altered, a result that is consistent with the findings from the collagen gel invasion assay. Thus, Cx43 is likely to act downstream of EMT by affecting cell migration behavior.

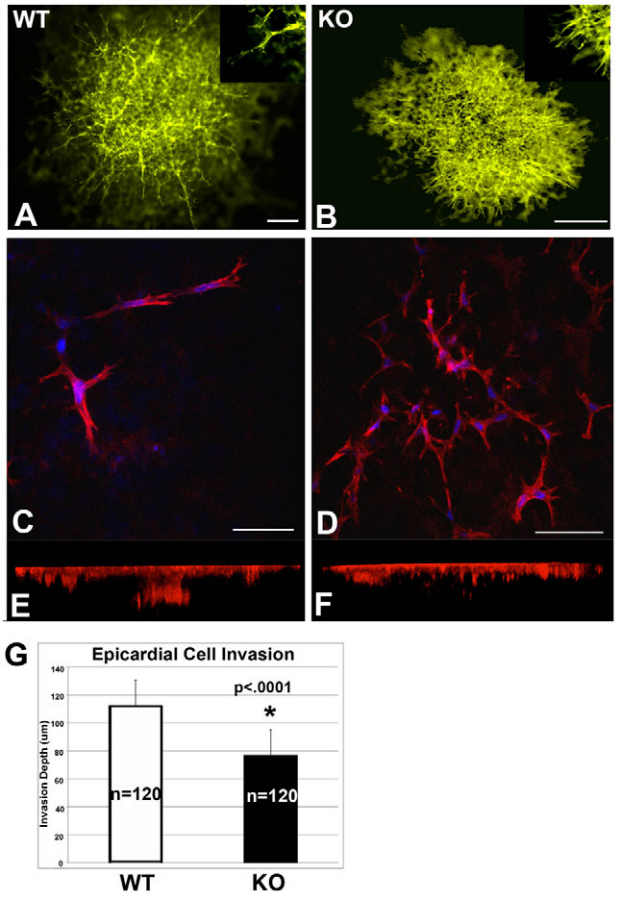

Fig. 4. Epicardial cell invasion in 3D collagen gel matrix. E11.5 epicardial cells were explanted on a 3D collagen gel matrix and then stained with rhodamine-conjugated phalloidin and DAPI to visualize epicardial cell invasion into the matrix. (**A**,**B**) Wild-type explants (A) exhibited organized outgrowths with long extended projections into the collagen gel matrix, but this was not observed in the Cx43 KO epicardial cells (B). (**C-F**) Confocal imaging of these collagen gel explants (shown along the *x*/*y* plane in C and D) was used to generate 3D reconstructions for measurement of cell invasion depth along the *z*-axis (E,F). (**G**) Measurements along the *z*-axes showed a significant decrease in the depth of cell invasion in the KO explants compared with wild type (*n*=6 explants per genotype, 120 cells measured for each). Scale bars: 250 μm in A,B; 50 μm in C; 75 μm in D.

Defects in directional cell migration and epicardial cell polarization

To examine whether there are changes in cell motile behavior in Cx43 KO epicardial cells, we carried out time-lapse video microscopy to examine epicardial cell migration in E11.5 epicardial explants. Measurements were made by tracing the migration paths of individual cells emerging from the epicardial explants. A total of 28 cells were thus analyzed from three wild-type embryos, together with 16 cells from six KO embryos. These studies showed that the wild-type epicardial cells migrated along relatively straight paths (Fig. 6A). By contrast, epicardial cells from the KO explants exhibited more tortuous migratory paths (Fig. 6B). Quantitative analysis of the cell tracing data showed that the KO epicardial cells

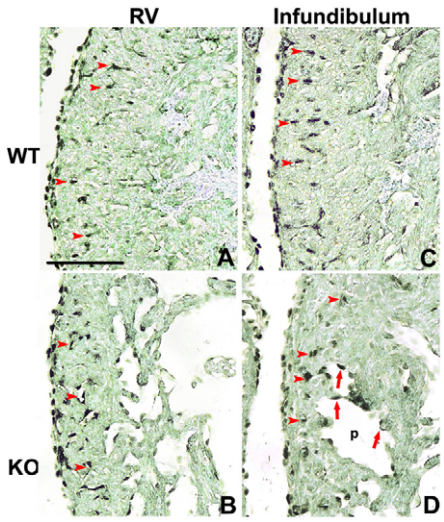

Fig. 5. Altered migration of EPDCs in the Cx43 KO heart. (**A-D**) Wt1 immunostaining of sections of E14.5 wild-type and Cx43 KO mouse hearts. In wild type (A,C), the invading EPDCs are aligned with the presumptive direction of cell migration into the heart (red arrowhead). This was not observed in the KO heart (B,D), where the Wt1-positive EPDCs showed a disorganized distribution. Note abundant Wt1-positive EPDCs (red arrows in D) lining the infundibular pouches (p) in the KO heart (D). RV, right ventricle; Infundibulum, infundibular region of the right ventricle. Scale bar: 100 μm.

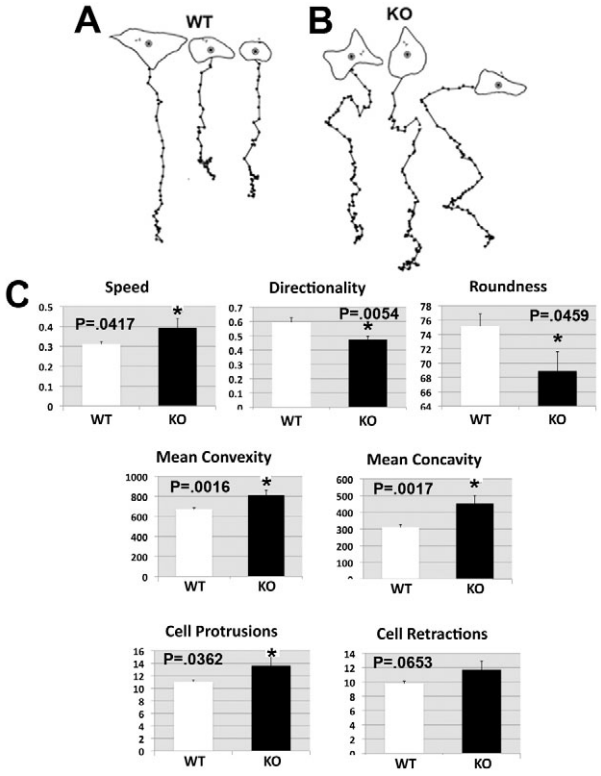

Fig. 6. Cx43 KO epicardial cells exhibit changes in cell migration and cell shape. (**A**,**B**) Time-lapse videomicroscopy and cell-tracing analyses showed straight migration paths for epicardial cells in the wild-type explants (A), but tortuous migration paths for epicardial cells in the KO explants (B). (**C**) Quantitative motion analysis showed a decrease in directional cell movement, and an increase in cell protrusions and retractions in KO explants compared with in wild type. A marked change in cell shape was also indicated by the decrease in cell roundness and increases in cell convexity and concavity.

migrated with increased speed, but decreased directionality, the latter being defined as the net migration distance divided by the total distance traveled (Fig. 6C). There was also increased cell protrusive activity, as indicated by the increased protrusion and retraction of cell processes (Fig. 6C). These changes in cell motile behavior were accompanied by dynamic changes in cell shape, including decreased roundness and increased convexity and concavity, measures of the complexity of cell shape (see Materials and methods; see also Fig. 6C).

Directional cell migration requires polarized alignment of the cytoskeleton and typically the microtubule organizing center (MTOC) and Golgi are positioned forward facing at the leading edge of the cell (Kupfer et al., 1983; Kupfer et al., 1982; Magdalena et al., 2003). In wild-type epicardial cells, immunostaining with an α-tubulin antibody delineated the tubulin cytoskeleton in conjunction with the MTOC, the latter being seen as a bright crescent-shaped structure (Fig. 7A). This structure was oriented towards the direction of cell migration, i.e. was forward facing, in wild-type epicardial cells, but in KO epicardial cells there was randomization in the orientation of the MTOC (Fig. 7A,B, graph). Parallel analysis using antibodies to visualize γ-tubulin, an essential component of MTOCs, and GM130, a Golgi marker colocalized with γ-tubulin, yielded similar findings (Fig. 7C,D, graphs). These results showed that the Cx43 KO epicardial cells were unable to establish the cell polarity required for directional cell migration.

Cx43 tubulin-binding domain is required for epicardial cell polarity

Changes in the tubulin cytoskeleton of Cx43 KO epicardial cells are of particular interest in light of previous studies showing Cx43 binding to tubulin via a juxtamembrane region in the carboxy terminus of Cx43 (Giepmans et al., 2001a; Giepmans et al., 2001b). To examine whether this region of Cx43 might be required for the normal regulation of cell polarity and directional cell migration, we generated a GFP-tagged Cx43 construct lacking amino acid residues 234-243 (Cx43dT). This peptide sequence, situated in the Cx43 juxtamembrane region required for tubulin binding, corresponds to a tubulin-binding motif (Giepmans et al., 2001a). As a control, we also generated a construct expressing full-length Cx43 fused in frame with GFP. It should be noted that both the full-length Cx43-GFP fusion protein and the Cx43-GFP construct with the entire carboxy terminus of Cx43 deleted have been shown to traffic to the cell surface and form functional gap junction plaques that mediate gap junction communication (Jordan et al., 1999; Omori and Yamasaki, 1999). These two Cx43-GFP fusion constructs and a control GFP-expressing plasmid were each transfected into epicardial explants, and time-lapse imaging was carried out to examine the affect on cell migration behavior.

The motile behaviors of cells expressing either GFP or the full-length Cx43-GFP fusion protein were indistinguishable from one another and were similar to that of non-transfected cells. By contrast, cells expressing the Cx43dT-GFP fusion protein exhibited increased cell protrusive activity, as indicated by increases in the extension and retraction of cell protrusions; this was accompanied by a reduction in roundness (Fig. 8E). These changes are reminiscent of those observed in the Cx43 KO epicardial cells (Fig. 6C). Immunostaining of the transfected cells with γ-tubulin to delineate the MTOC showed

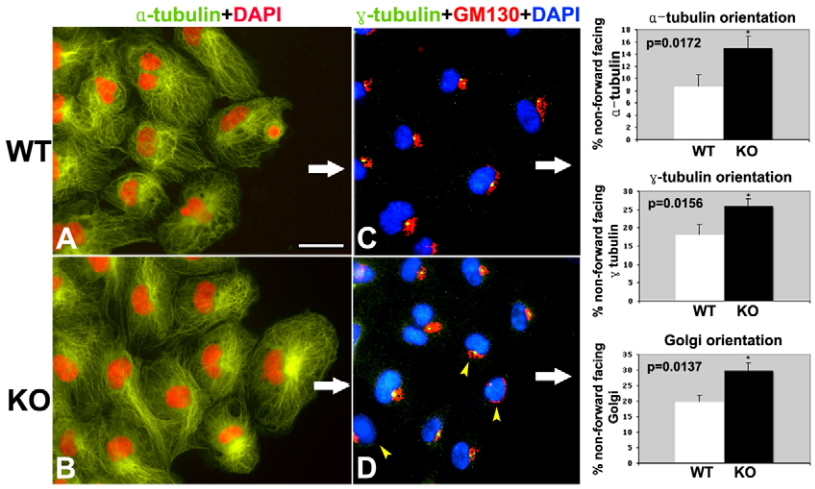

Fig. 7. Defect in the specification of cell polarity in Cx43 KO epicardial cells. (**A-D**) Epicardial cells from E11.5 explant cultures were immunostained with antibodies to α-tubulin (A,B), or γ-tubulin and the Golgi GM130 marker (C,D) to visualize the MTOC. α-Tubulin staining exhibited an intensely stained crescent-shaped structure that corresponds to the MTOC. In wild-type cells, most of the MTOC are forward facing, i.e. situated in the leading edge of the cell (white arrow indicates the direction of cell migration). The microtubules were also observed to align with the direction of cell migration. By contrast, in the Cx43 KO explants, the MTOC and the microtubule cytoskeleton were often not aligned with the direction of cell migration (B). A similar result was obtained when γ-tubulin and GM130 antibodies were used to track the positioning of the MTOC in wild-type (C) and KO epicardial cells (D). The quantitative analysis is shown in the bar graphs to the right. Red and blue staining in A,B and C,D, respectively, corresponds to DAPI staining. Scale bar: 50 μm.

that the MTOC was not aligned with the direction of cell migration in the Cx43dT-expressing cells (Fig. 8C,D), as nearly 70% of the MTOCs in these transfected cells were not forward facing (Fig. 8E). By contrast, cells expressing full-length Cx43 exhibited MTOCs that were well aligned with the direction of cell migration (Fig. 8A,B), with only 10% non-forward facing cells (Fig. 8E). Similar results were observed for the GFP transfected cells. These findings indicate that the putative tubulin-binding domain in Cx43 is required for epicardial cell polarity.

Defects in remodeling of the coronary vascular plexuses

To evaluate the developmental effects resulting from the epicardial cytoskeletal changes and cell polarity defects, we examined the emergence of the primitive coronary vascular plexuses by whole-mount Pecam staining of E11.5 hearts (Fig. 9). The coronary vascular networks in the KO hearts exhibited a more irregular and disorganized pattern than did the wild-type hearts, with ectopic vessels seen to criss-cross the forming vascular plexuses (arrowheads in Fig. 9D). There was an increase in the caliper of ectopic vessels in the anterior surface of the heart (Fig. 9F). Quantitative analysis of the Pecam-stained E11.5 hearts showed a reduction in the density of the primitive coronary vascular networks in the KO versus the wild-type hearts (Fig. 9G-I). These findings suggest a defect in remodeling of the primitive coronary vascular plexuses in the Cx43 KO mouse heart.

Perturbation in myocardialization of the outflow tract

EMT and cell migration has also been shown to play an essential role in muscularization of the outflow tract septum via infiltration of myocardializing cells into cushion tissue (Phillips et al., 2005; Phillips et al., 2007). This process of myocardialization is regulated by *Vangl2* and other genes in the noncanonical Wnt planar cell polarity pathway (PCP), and entails reorganization of the actin cytoskeleton to form stress fibers aligned with the direction of cell migration and polarized cell invasion into the outflow septum (Phillips et al., 2005; Phillips et al., 2007). To examine whether conotruncal pouch formation in the KO mouse heart could arise from a defect in EMT and polarized cell migration required for myocardialization of the outflow tract, we examined muscularization of the outflow septum in histological sections immunostained for sarcomeric actin (Fig. 10). In wild-type hearts, cardiomyocytes in the outflow tract exhibited elongate finger-like projections aligned with the apparent direction of polarized cell invasion into the outflow cushion tissue (Fig. 10A). By contrast, in the KO heart, the myocardializing cells were disorganized and exhibited few myocardial cell projections into the outflow tract cushion tissue (Fig. 10B). This defect in myocardialization resulted in a delay in muscularization of the outflow septum in the KO mouse heart. Thus, there were still large areas of the outflow septum not yet muscularized in the KO heart at E14.5 when most of the outflow septum in the wild-type heart was already muscularized (Fig. 10C,D). As this defect in myocardialization is reminiscent of defects observed in Vangl2 KO mice and other mutants with defects in PCP signaling, we carried out real-time PCR analysis to further examine the expression of *Vangl2* and other genes of the noncanonical Wnt planar cell polarity (PCP) pathway that have recently been shown to regulate myocardialization of the outflow septum (Phillips et al., 2005; Phillips et al., 2007). However, no significant changes were detected (see Table S1 in the supplementary material).

DISCUSSION

Our studies show that Cx43 deficiency altered the cytoarchitecture of the epicardium and the EPDCs. The presence of epicardial blisters in the KO hearts suggests possible defects in epicardial EMT and the deployment of the EPDCs. Analysis of epicardial explants suggests that Cx43 deficiency causes a disruption of epicardial cell-cell adhesion in conjunction with the redistribution of ZO-1 to the cytoplasm. This was associated with a reduction in the size of focal adhesion plaques that mediate cell-matrix attachment. Together, these changes could facilitate the disengagement of cells from the epicardial sheet and promote formation of the epicardial blisters. Analysis of Wt1-positive infiltrating EPDCs showed that EPDCs in the KO heart failed to exhibit the directional alignment seen in wild-type hearts. The KO heart also showed a defect in remodeling of the primitive coronary vascular plexuses, with an abundance of ectopic fine coronary vessels found intermingling in a network of vascular plexuses of reduced density. Together, these observations suggest Cx43 deficiency causes abnormal deployment of the EPDCs and the coronary vascular progenitors.

By using a three-dimensional collagen gel invasion assay, we showed that the Cx43 KO epicardial cells underwent EMT, but they were less invasive and failed to coalesce into the long thin vessel-

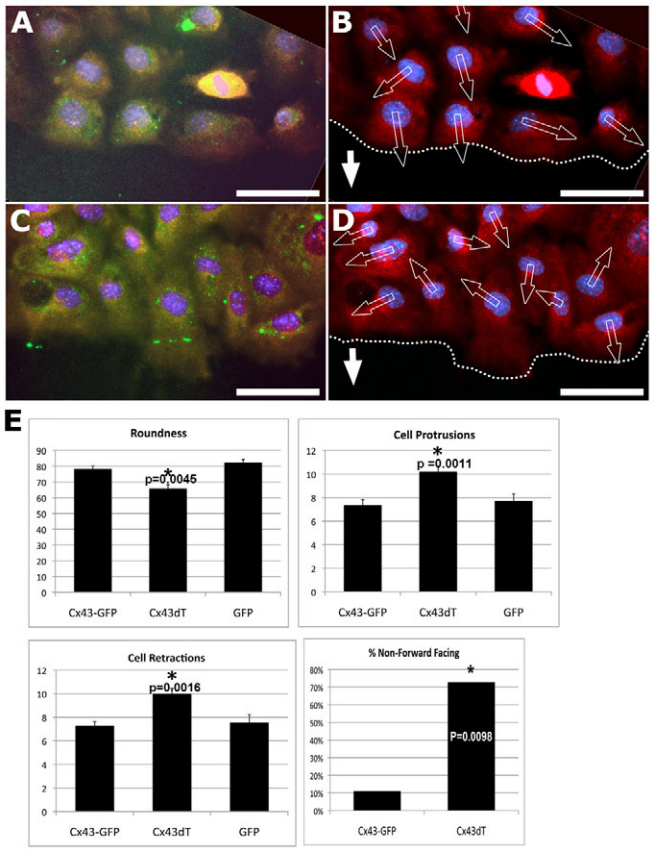

Fig. 8. Cx43 tubulin-binding domain is required for epicardial cell polarity. (**A-D**) E11.5 epicardial explants were transfected with plasmids expressing either wild-type Cx43 fused with GFP (A,B) or Cx43 with the putative tubulin-binding domain deleted (Cx43dT) and fused with GFP (C,D). Transfection of GFP alone was also carried out as another control. Transfected cells were identified by GFP expression (A,C). Staining with γ-tubulin antibody (B,D), shown by the red dot enclosed by the white arrow, delineated the orientation of the MTOC. (**E**) In Cx43 KO epicardial cells, the MTOC failed to align with the direction of cell migration, as indicated by a very high percentage of non-forward-facing MTOC. Quantitative motion analysis revealed a significant increase in the extension and retraction of cell protrusions and in roundness of the Cx43dT cells compared to the Cx43 transfected cells (*P*-value indicated in graph). Significant differences were also observed when Cx43dT was compared with the GFP transfected cells (roundness, *P*=0.0001; cell protrusions, *P*=0.0261; cell retractions, *P*=0.0255). Scale bar: 50 μm.

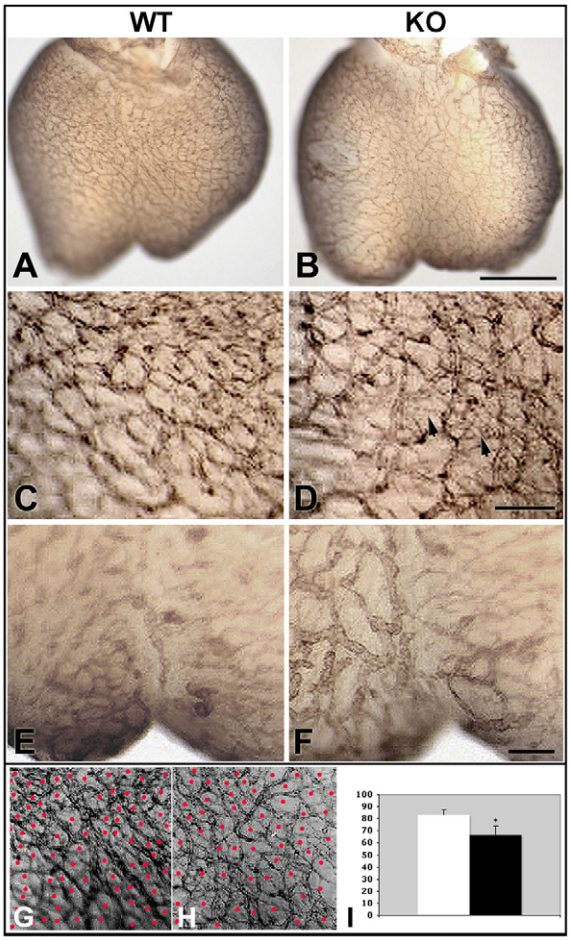

Fig. 9. Defect in remodeling of the primitive coronary vascular plexus in Cx43 KO mice. (**A-H**) Whole-mount Pecam immunostaining of E13.5 hearts shows the distribution of the coronary vascular plexuses in wild-type (A,C,E,G; WT) and Cx43 KO (B,D,F,H; KO) mouse hearts. (A-D) Wild-type (A,C) and Cx43 KO (B,D) mouse hearts show a network of coronary vascular plexuses. In enlarged views, the KO (D), but not the wild-type (C) heart shows fine vessels (arrowheads) criss-crossing the major coronary vascular network. (F) Magnified anterior view of Pecam-stained Cx43 KO (F) heart shows abnormally enlarged vessels near the apex. (E) Similar view of a Pecam-stained heart from a wild-type littermate. (G,H) Enlarged images of the hearts in A and B with red dots showing the scoring of vascular network. The results of this analysis, plotted in **I**, show a reduction in the density of the coronary vascular network in the KO (H, black bar in I) when compared wih wild-type (G, white bar in I) hearts. Scale bars: 50 μm in B (same as A); 10 μm in D and F (C,D and E,F are same magnification).

like projections seen in the wild-type explants. Although no changes were detected in the expression of genes known to regulate EMT, we found marked changes in the actin and tubulin cytoskeleton in KO epicardial explants. This was associated with randomized positioning of the MTOC, which would suggest an underlying defect in the specification of cell polarity in the Cx43 KO epicardial cells. Consistent with this, video microscopy and quantitative motion analysis showed a reduction in the directionality of cell locomotion in the KO epicardial explants This was associated with an increase in cell protrusive activity and alterations in cell shape. We previously showed similar changes in cell motility in conjunction with neural crest cell migration defects in the Cx43 KO mouse embryo (Xu et al., 2006). As observed with the Cx43 KO epicardial cells, Cx43 KO cardiac neural crest cells exhibited a defect in cell polarity (Xu et al., 2006).

As the specification of cell polarity is essential for directional cell migration, this could account for the anomalous migration of the EPDCs and the disruption in the dynamic remodeling of the primitive coronary vascular plexuses. Defects in EDPC migration could underlie the ectopic distribution of endothelial and vascular smooth muscle cells in the Cx43 KO mouse heart (Walker et al., 2005). The epicardial blisters seen in the KO heart are reminiscent of polycystic kidney disease, where cyst formation arises from defects in the specification of cell polarity via the disruption of PCP signaling

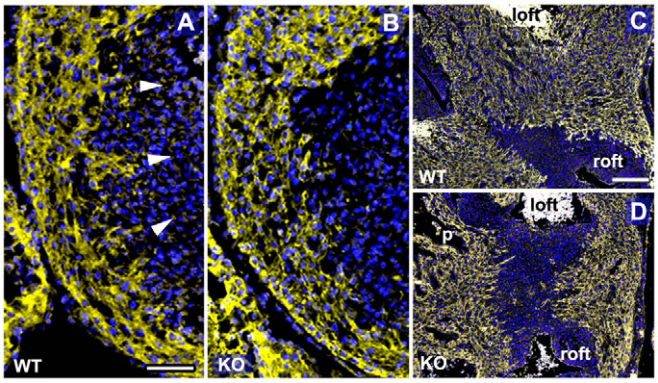

Fig. 10. Defect in cardiomyocytes during myocardialization. (**A**) Histological sections immunostained for sarcomeric actin (yellow) show myocardial invasion and muscularization of the outflow tract in the wild-type E13.5 heart. Cardiomyocytes with polarized morphology, organized in finger-like projections (white arrowheads in panel A), are observed to extend into the flanking cushion tissue. (**B**) By contrast, in the Cx43 KO heart, cariomyocytes failed to show such distinct polarized orientation. (**C**,**D**) A day later at E14.5, most of the outflow tract mesenchyme in wild-type hearts was muscularized (C), but in the E14.5 KO heart (D) there were substantial regions of the outflow tract cushion tissue that were devoid of cardiomyocytes. loft, left outflow tract; roft, right outflow tract; p, pouch. Scale bar: 100 μm in A; 200 μm in C.

(Montcouquiol, 2007; Saburi et al., 2008). We note that *Vangl2* and *Scrib*, core components of the PCP pathway, have been shown to play an essential role in myocardialization of the outflow tract (Phillips et al., 2005; Phillips et al., 2007). In the Cx43 KO mouse heart, outflow tract myocardialization was delayed, probably because of a defect in polarized migration of the myocardializing cells. *Vangl2* was also recently reported to exert non-cell-autonomous effects on the formation of the coronary vasculature (Phillips et al., 2008). However, real-time PCR analysis showed no change in transcript expression levels for several genes in the noncanonical Wnt-PCP pathway in the Cx43 KO heart. The delay in muscularization of the outflow mesenchyme in the Cx43 KO mouse is most evident at E14.5, the developmental stage when the conotruncal pouches are first distinctly visible. The delay in myocardialization together with the anomalous migration of EPDCs could together contribute to formation of the conotruncal pouches in the Cx43 KO mouse heart. We note that Wt1-expressing presumptive EPDCs were observed in abundance in the infundibular pouches.

We showed that the modulation of cell polarity by Cx43 requires amino acid residues 234-243 in the juxtamembrane region of the carboxy terminus of Cx43. This peptide sequence contains a tubulin-binding motif (residues underlined, ^{234}KGVKDRVKGK^{243}) (Giepmans et al., 2001a; Giepmans et al., 2001b). Previous studies by Giepmans et al. with various deletion constructs showed that amino acids spanning these residues are required for Cx43 binding to tubulin (Giepmans et al., 2001a; Giepmans et al., 2001b). Our studies showed that expression of the Cx43dT construct in epicardial cells caused cell polarity defects similar to those seen in the Cx43 KO epicardial explants. Thus, epicardial cells expressing the Cx43dT construct failed to orient the MTOC with the direction of cell migration, and these cells exhibited increased cell protrusive activity in conjunction with a decrease in roundness. As the transfected explants were from wild-type embryos that express endogenous Cx43, these results would suggest the Cx43dT construct exerted dominant-negative effects via Cx43 oligomerized in hemichannels or gap junction plaques.

Although gap junction proteins are predominantly thought of as membrane channels that mediate the intercellular movement of ions and small signaling molecules, connexins also have been shown to exert channel-independent effects via processes involving protein-protein interactions (Wei et al., 2004; Scemes, 2008). This might involve protein partners that play a role in the assembly and turnover of junctional complexes, and proteins that regulate the cytoskeleton (Duffy et al., 2002; Prochnow and Dermietzel, 2008; Wei et al., 2005; Wei et al., 2004; Xu et al., 2006; Xu et al., 2001). In addition to tubulin binding (Dai et al., 2007; Giepmans et al., 2001a; Giepmans et al., 2001b; Guo et al., 2003; Johnson et al., 2002; Shaw et al., 2007; Thomas et al., 2001), Cx43 has also been shown to bind ZO-1 (Barker et al., 2002; Giepmans and Moolenaar, 1998), which might explain the redistribution of ZO-1 to the cytoplasm in Cx43 KO epicardial cells. In some cell types, Cx43 is observed to traffic and colocalize with cadherins (Li et al., 2008; Nambara et al., 2007; Wei et al., 2005; Xu et al., 2001).

Overall, our findings suggest that the role of Cx43 in heart development is centered on the regulation of cell polarity, a process that might involve Cx43-tubulin interactions. Mechanistic insights into the regulation of microtubule dynamics and cell polarity by Cx43 will require further studies in the future with real-time dynamic imaging using total internal reflection fluorescence (TIRF) and spinning disk confocal microscopy. Biochemical analysis also will be needed to elucidate how Cx43 binding with tubulin might affect microtubule assembly and turnover. These studies may shed light on the intriguing possibility that Cx43 might have channel-independent functions.

Acknowledgements
We thank Dr Raymond Runyan for helpful advice on the 3D collagen gel assay, Chris Combs (NHLBI Light Microscopy Core Facility) for help with confocal imaging and Peter Yang for critical reading of the manuscript. D.Y.R. was funded in part by a Ruth L. Kirschstein National Research Service Award. Supported by grants from NIH ZO1-HL005701 to C.W.L. Deposited in PMC for release after 12 months.

Supplementary material
Supplementary material for this article is available at
http://dev.biologists.org/cgi/content/full/136/18/3185/DC1

References
Barker, R. J., Price, R. L. and Gourdie, R. G. (2002). Increased association of ZO-1 with connexin43 during remodeling of cardiac gap junctions. *Circ. Res.* **90**, 317-324.
Clauss, S. B., Walker, D. L., Kirby, M. L., Schimel, D. and Lo, C. W. (2006). Patterning of coronary arteries in wildtype and connexin43 knockout mice. *Dev. Dyn.* **235**, 2786-2794.
Dai, P., Nakagami, T., Tanaka, H., Hitomi, T. and Takamatsu, T. (2007). Cx43 mediates TGF-beta signaling through competitive Smads binding to microtubules. *Mol. Biol. Cell* **18**, 2264-2273.
Dettman, R. W., Denetclaw, W., Jr, Ordahl, C. P. and Bristow, J. (1998). Common epicardial origin of coronary vascular smooth muscle, perivascular fibroblasts, and intermyocardial fibroblasts in the avian heart. *Dev. Biol.* **193**, 169-181.
Duffy, H. S., Delmar, M. and Spray, D. C. (2002). Formation of the gap junction nexus: binding partners for connexins. *J. Physiol. Paris* **96**, 243-249.
Ewart, J. L., Cohen, M. F., Meyer, R. A., Huang, G. Y., Wessels, A., Gourdie, R. G., Chin, A. J., Park, S. M., Lazatin, B. O., Villabon, S. et al. (1997). Heart and neural tube defects in transgenic mice overexpressing the Cx43 gap junction gene. *Development* **124**, 1281-1292.
Giepmans, B. N. and Moolenaar, W. H. (1998). The gap junction protein connexin43 interacts with the second PDZ domain of the zona occludens-1 protein. *Curr. Biol.* **8**, 931-934.
Giepmans, B. N., Verlaan, I., Hengeveld, T., Janssen, H., Calafat, J., Falk, M. M. and Moolenaar, W. H. (2001a). Gap junction protein connexin-43 interacts directly with microtubules. *Curr. Biol.* **11**, 1364-1368.
Giepmans, B. N., Verlaan, I. and Moolenaar, W. H. (2001b). Connexin-43 interactions with ZO-1 and alpha- and beta-tubulin. *Cell Commun. Adhes.* **8**, 219-223.
Gittenberger-de Groot, A. C., Vrancken Peeters, M. P., Mentink, M. M., Gourdie, R. G. and Poelmann, R. E. (1998). Epicardium-derived cells

contribute a novel population to the myocardial wall and the atrioventricular cushions. *Circ. Res.* **82**, 1043-1052.
Goldberg, G. S., Moreno, A. P. and Lampe, P. D. (2002). Gap junctions between cells expressing connexin 43 or 32 show inverse permselectivity to adenosine and ATP. *J. Biol. Chem.* **277**, 36725-36730.
Guo, Y., Martinez-Williams, C. and Rannels, D. E. (2003). Gap junction-microtubule associations in rat alveolar epithelial cells. *Am. J. Physiol. Lung Cell Mol. Physiol.* **285**, L1213-L1221.
Hood, L. C. and Rosenquist, T. H. (1992). Coronary artery development in the chick: origin and deployment of smooth muscle cells, and the effects of neural crest ablation. *Anat. Rec.* **234**, 291-300.
Huang, G. Y., Cooper, E. S., Waldo, K., Kirby, M. L., Gilula, N. B. and Lo, C. W. (1998a). Gap junction-mediated cell-cell communication modulates mouse neural crest migration. *J. Cell Biol.* **143**, 1725-1734.
Huang, G. Y., Wessels, A., Smith, B. R., Linask, K. K., Ewart, J. L. and Lo, C. W. (1998b). Alteration in connexin 43 gap junction gene dosage impairs conotruncal heart development. *Dev. Biol.* **198**, 32-44.
Imamura, Y., Itoh, M., Maeno, Y., Tsukita, S. and Nagafuchi, A. (1999). Functional domains of alpha-catenin required for the strong state of cadherin-based cell adhesion. *J. Cell Biol.* **144**, 1311-1322.
Itoh, M., Nagafuchi, A., Moroi, S. and Tsukita, S. (1997). Involvement of ZO-1 in cadherin-based cell adhesion through its direct binding to alpha catenin and actin filaments. *J. Cell Biol.* **138**, 181-192.
Johnson, R. G., Meyer, R. A., Li, X. R., Preus, D. M., Tan, L., Grunenwald, H., Paulson, A. F., Laird, D. W. and Sheridan, J. D. (2002). Gap junctions assemble in the presence of cytoskeletal inhibitors, but enhanced assembly requires microtubules. *Exp. Cell Res.* **275**, 67-80.
Jordan, K., Solan, J. L., Dominguez, M., Sia, M., Hand, A., Lampe, P. D. and Laird, D. W. (1999). Trafficking, assembly, and function of a connexin43-green fluorescent protein chimera in live mammalian cells. *Mol. Biol. Cell* **10**, 2033-2050.
Kanno, S. and Saffitz, J. E. (2001). The role of myocardial gap junctions in electrical conduction and arrhythmogenesis. *Cardiovasc. Pathol.* **10**, 169-177.
Kupfer, A., Louvard, D. and Singer, S. J. (1982). Polarization of the Golgi apparatus and the microtubule-organizing center in cultured fibroblasts at the edge of an experimental wound. *Proc. Natl. Acad. Sci. USA* **79**, 2603-2607.
Kupfer, A., Dennert, G. and Singer, S. J. (1983). Polarization of the Golgi apparatus and the microtubule-organizing center within cloned natural killer cells bound to their targets. *Proc. Natl. Acad. Sci. USA* **80**, 7224-7228.
Kwee, L., Baldwin, H. S., Shen, H. M., Stewart, C. L., Buck, C., Buck, C. A. and Labow, M. A. (1995). Defective development of the embryonic and extraembryonic circulatory systems in vascular cell adhesion molecule (VCAM-1) deficient mice. *Development* **121**, 489-503.
Lauf, U., Giepmans, B. N., Lopez, P., Braconnot, S., Chen, S. C. and Falk, M. M. (2002). Dynamic trafficking and delivery of connexons to the plasma membrane and accretion to gap junctions in living cells. *Proc. Natl. Acad. Sci. USA* **99**, 10446-10451.
Li, W. E., Waldo, K., Linask, K. L., Chen, T., Wessels, A., Parmacek, M. S., Kirby, M. L. and Lo, C. W. (2002). An essential role for connexin43 gap junctions in mouse coronary artery development. *Development* **129**, 2031-2042.
Li, Z., Zhou, Z. and Donahue, H. J. (2008). Alterations in Cx43 and OB-cadherin affect breast cancer cell metastatic potential. *Clin. Exp. Metastasis* **25**, 265-272.
Magdalena, J., Millard, T. H. and Machesky, L. M. (2003). Microtubule involvement in NIH 3T3 Golgi and MTOC polarity establishment. *J. Cell Sci.* **116**, 743-756.
Manner, J. (1999). Does the subepicardial mesenchyme contribute myocardioblasts to the myocardium of the chick embryo heart? A quail-chick chimera study tracing the fate of the epicardial primordium. *Anat. Rec.* **255**, 212-226.
Mikawa, T. and Gourdie, R. G. (1996). Pericardial mesoderm generates a population of coronary smooth muscle cells migrating into the heart along with ingrowth of the epicardial organ. *Dev. Biol.* **174**, 221-232.
Montcouquiol, M. (2007). Planar polarity in mammals: similarity and divergence with Drosophila Melanosgaster. *J. Soc. Biol.* **201**, 61-67.
Munoz-Chapuli, R., Gonzalez-Iriarte, M., Carmona, R., Atencia, G., Macias, D. and Perez-Pomares, J. M. (2002). Cellular precursors of the coronary arteries. *Tex. Heart Inst. J.* **29**, 243-249.
Nambara, C., Kawasaki, Y. and Yamasaki, H. (2007). Role of the cytoplasmic loop domain of Cx43 in its intracellular localization and function: possible interaction with cadherin. *J. Membr. Biol.* **217**, 63-69.
Nobes, C. D. and Hall, A. (1999). Rho GTPases control polarity, protrusion, and adhesion during cell movement. *J. Cell Biol.* **144**, 1235-1244.
Omori, Y. and Yamasaki, H. (1999). Gap junction proteins connexin32 and connexin43 partially acquire growth-suppressive function in HeLa cells by deletion of their C-terminal tails. *Carcinogenesis* **20**, 1913-1918.
Perez-Pomares, J. M., Phelps, A., Sedmerova, M., Carmona, R., Gonzalez-Iriarte, M., Munoz-Chapuli, R. and Wessels, A. (2002). Experimental studies on the spatiotemporal expression of WT1 and RALDH2 in the embryonic avian heart: a model for the regulation of myocardial and valvuloseptal development by epicardially derived cells (EPDCs). *Dev. Biol.* **247**, 307-326.
Phillips, H. M., Murdoch, J. N., Chaudhry, B., Copp, A. J. and Henderson, D. J. (2005). Vangl2 acts via RhoA signaling to regulate polarized cell movements during development of the proximal outflow tract. *Circ. Res.* **96**, 292-299.
Phillips, H. M., Rhee, H. J., Murdoch, J. N., Hildreth, V., Peat, J. D., Anderson, R. H., Copp, A. J., Chaudhry, B. and Henderson, D. J. (2007). Disruption of planar cell polarity signaling results in congenital heart defects and cardiomyopathy attributable to early cardiomyocyte disorganization. *Circ. Res.* **101**, 137-145.
Phillips, H. M., Hildreth, V., Peat, J. D., Murdoch, J. N., Kobayashi, K., Chaudhry, B. and Henderson, D. J. (2008). Non-cell-autonomous roles for the planar cell polarity gene Vangl2 in development of the coronary circulation. *Circ. Res.* **102**, 615-623.
Poelmann, R. E., Gittenberger-de Groot, A. C., Mentink, M. M., Bokenkamp, R. and Hogers, B. (1993). Development of the cardiac coronary vascular endothelium, studied with antiendothelial antibodies, in chicken-quail chimeras. *Circ. Res.* **73**, 559-568.
Polette, M., Mestdagt, M., Bindels, S., Nawrocki-Raby, B., Hunziker, W., Foidart, J. M., Birembaut, P. and Gilles, C. (2007). Beta-catenin and ZO-1: shuttle molecules involved in tumor invasion-associated epithelial-mesenchymal transition processes. *Cells Tissues Organs* **185**, 61-65.
Prochnow, N. and Dermietzel, R. (2008). Connexons and cell adhesion: a romantic phase. *Histochem. Cell Biol.* **130**, 71-77.
Reaume, A. G., de Sousa, P. A., Kulkarni, S., Langille, B. L., Zhu, D., Davies, T. C., Juneja, S. C., Kidder, G. M. and Rossant, J. (1995). Cardiac malformation in neonatal mice lacking connexin43. *Science* **267**, 1831-1834.
Runyan, R. B. and Markwald, R. R. (1983). Invasion of mesenchyme into three-dimensional collagen gels: a regional and temporal analysis of interaction in embryonic heart tissue. *Dev. Biol.* **95**, 108-114.
Saburi, S., Hester, I., Fischer, E., Pontoglio, M., Eremina, V., Gessler, M., Quaggin, S. E., Harrison, R., Mount, R. and McNeill, H. (2008). Loss of Fat4 disrupts PCP signaling and oriented cell division and leads to cystic kidney disease. *Nat. Genet.* **40**, 1010-1015.
Saez, J. C., Berthoud, V. M., Branes, M. C., Martinez, A. D. and Beyer, E. C. (2003). Plasma membrane channels formed by connexins: their regulation and functions. *Physiol. Rev.* **83**, 1359-1400.
Scemes, E. (2008). Modulation of astrocyte P2Y1 receptors by the carboxyl terminal domain of the gap junction protein Cx43. *Glia* **56**, 145-153.
Shaw, R. M., Fay, A. J., Puthenveedu, M. A., von Zastrow, M., Jan, Y. N. and Jan, L. Y. (2007). Microtubule plus-end-tracking proteins target gap junctions directly from the cell interior to adherens junctions. *Cell* **128**, 547-560.
Stites, J., Wessels, D., Uhl, A., Egelhoff, T., Shutt, D. and Soll, D. R. (1998). Phosphorylation of the Dictyostelium myosin II heavy chain is necessary for maintaining cellular polarity and suppressing turning during chemotaxis. *Cell Motil. Cytoskel.* **39**, 31-51.
Soll, D. R. (1995). The use of computers in understanding how animal cells crawl. *Int. Rev. Cytol.* **163**, 43-104.
Sullivan, R. and Lo, C. W. (1995). Expression of a connexin 43/beta-galactosidase fusion protein inhibits gap junctional communication in NIH3T3 cells. *J. Cell Biol.* **130**, 419-429.
Thomas, T., Jordan, K. and Laird, D. W. (2001). Role of cytoskeletal elements in the recruitment of Cx43-GFP and Cx26-YFP into gap junctions. *Cell Commun. Adhes.* **8**, 231-236.
Viragh, S. and Challice, C. E. (1981). The origin of the epicardium and the embryonic myocardial circulation in the mouse. *Anat. Rec.* **201**, 157-168.
Vrancken Peeters, M. P., Gittenberger-de Groot, A. C., Mentink, M. M. and Poelmann, R. E. (1999). Smooth muscle cells and fibroblasts of the coronary arteries derive from epithelial-mesenchymal transformation of the epicardium. *Anat. Embryol. (Berl.)* **199**, 367-378.
Waldo, K. L., Kumiski, D. H. and Kirby, M. L. (1994). Association of the cardiac neural crest with development of the coronary arteries in the chick embryo. *Anat. Rec.* **239**, 315-331.
Walker, D. L., Vacha, S. J., Kirby, M. L. and Lo, C. W. (2005). Connexin43 deficiency causes dysregulation of coronary vasculogenesis. *Dev. Biol.* **284**, 479-498.
Wei, C. J., Xu, X. and Lo, C. W. (2004). Connexins and cell signaling in development and disease. *Annu. Rev. Cell Dev. Biol.* **20**, 811-838.
Wei, C. J., Francis, R., Xu, X. and Lo, C. W. (2005). Connexin43 associated with an N-cadherin-containing multiprotein complex is required for gap junction formation in NIH3T3 cells. *J. Biol. Chem.* **280**, 19925-19936.
Xu, X., Li, W. E., Huang, G. Y., Meyer, R., Chen, T., Luo, Y., Thomas, M. P., Radice, G. L. and Lo, C. W. (2001). Modulation of mouse neural crest cell motility by N-cadherin and connexin 43 gap junctions. *J. Cell Biol.* **154**, 217-230.
Xu, X., Francis, R., Wei, C. J., Linask, K. L. and Lo, C. W. (2006). Connexin 43-mediated modulation of polarized cell movement and the directional migration of cardiac neural crest cells. *Development* **133**, 3629-3639.
Yang, J. T., Rayburn, H. and Hynes, R. O. (1995). Cell adhesion events mediated by alpha 4 integrins are essential in placental and cardiac development. *Development* **121**, 549-560.
Zhou, B., Ma, Q., Rajagopal, S., Wu, S. M., Domian, I., Rivera-Feliciano, J., Jiang, D., von Gise, A., Ikeda, S., Chien, K. R. et al. (2008). Epicardial progenitors contribute to the cardiomyocyte lineage in the developing heart. *Nature* **454**, 109-113.